J|A|C|S ARTICLES

Published on Web 10/06/2010

Molecular Hydrogen "Pairing" Interaction in a Metal Organic Framework System with Unsaturated Metal Centers (MOF-74)

Nour Nijem,[†] Jean-François Veyan,[†] Lingzhu Kong,[‡] Haohan Wu,[§] Yonggang Zhao,[§] Jing Li,[§] David C. Langreth,[‡] and Yves J. Chabal*,[†]

Department of Materials Science & Engineering, University of Texas at Dallas, Richardson, Texas 75080, United States, Department of Physics and Astronomy, Rutgers University, 610 Taylor Road, Piscataway, New Jersey 08854, United States, and Department of Chemistry and Chemical Biology, Rutgers University, 610 Taylor Road, Piscataway, New Jersey 08854, United States

Received June 5, 2010; E-mail: chabal@utdallas.edu

Abstract: Infrared (IR) absorption spectroscopy measurements of molecular hydrogen in MOF-74-M (M = metal center) are performed as a function of temperature and pressure [to 45 kTorr (60 bar) at 300 K, and at lower pressures in the 20−200 K range] to investigate the nature of H_2 interactions with the unsaturated metal centers. A small shift (~ -30 cm^{-1} with respect to the unperturbed H_2 molecule) is observed for the internal stretch frequency of H_2 molecules adsorbed on the metal site at low loading. This finding is in contrast to much larger shifts (~ -70 cm^{-1}) observed in previous studies of MOFs with unsaturated metal centers (including MOF-74) and the general assumption that H_2 stretch shifts depend on adsorption energies (FitzGerald et al., *Phys. Rev. B* **2010**, *81*, 104305). We show that larger shifts (~ -70 cm^{-1}) do occur, but only when the next available site ("oxygen" site) is occupied. This larger shift originates from H_2-H_2 interactions on neighboring sites of the same pore, consistent with the short distance between H_2 in these two sites $\sim$2.6 Å derived from an analysis of neutron diffraction experiments of D_2-D_2 at 4 K (Liu et al., *Langmuir* **2008**, *24*, 4772−4777). Our results at 77 K and low loading can be explained by a diffusion barrier against pair disruption, which should be enhanced by this interaction. Calculations indicate that the vibrational shifts do not correlate with binding energies and are instead very sensitive to the environment (interaction potential and H_2-H_2 interactions), which complicates the use of variable temperature IR methods to calculate adsorption energies of specific adsorption sites.

1. Introduction

Metal organic framework (MOF) materials are being considered for many applications including gas separation and storage, catalysis, and sensing.[1−21] Their structure is comprised of metal or metal oxide clusters that are connected via organic ligands to form 3D porous structures. Hydrogen storage by physisorption is particularly promising in these materials due to their high surface area and porosity. The flexibility and relative ease to generate a variety of structures with controllable pore sizes simply by changing the organic linker and/or metal center is an important attribute of these materials.[16,22−24] The major drawback of such systems for hydrogen storage applications is their weak H_2 binding energies currently of $\sim$7−10 kJ/mol, that is, well below the 20−25 kJ/mol required for on-board applications.[25] Therefore, strategies to increase H_2 binding energies have been the focal point of numerous studies. Routes such as post synthetic modification of MOFs are being considered, incorporating reactive metal centers and exploration of spill over mechanisms.[26−32]

To investigate such complex mechanisms, it is first necessary to understand the interactions of H_2 in MOFs containing unsaturated metal centers that present high binding energy sites. Such structures have shown enhanced hydrogen uptakes and higher heats of hydrogen adsorption ($\sim$10 kJ/mol) as compared to saturated metal center MOFs ($\sim$4−5 kJ/mol) due to the higher adsorption energy metal sites.[33,6,34−40] Recent studies on

[†] University of Texas at Dallas.
[‡] Department of Physics and Astronomy, Rutgers University.
[§] Department of Chemistry and Chemical Biology, Rutgers University.

(1) Bae, Y. S.; Farha, O. K.; Hupp, J. T.; Snurr, R. Q. *J. Mater. Chem.* **2009**, *19*, 2131–2134.
(2) Kuppler, R. J.; Timmons, D. J.; Fang, Q.-R.; Li, J.-R.; Makal, T. A.; Young, M. D.; Yuan, D.; Zhao, D.; Zhuang, W.; Zhou, H.-C. *Coord. Chem. Rev.* **2009**, *253*, 3042–3066.
(3) Pan, L. H.; Olson, D. R.; Ciemnolonski, L.; Heddy, R.; Li, J. *Angew. Chem., Int. Ed.* **2006**, *45*, 616–619.
(4) Wang, D. E.; Deng, K. J.; Lv, K. L.; Wang, C. G.; Wen, L. L.; Li, D. F. *CrystEngComm* **2009**, *11*, 1442–1450.
(5) Dietzel, P. D. C.; Besikiotis, V.; Blom, R. *J. Mater. Chem.* **2009**, *19*, 7362–7370.
(6) Zhao, D.; Yuan, D. Q.; Zhou, H. C. *Energy Environ. Sci.* **2008**, *1*, 222–235.
(7) Chen, B.; Yang, Y.; Zapata, F.; Lin, G.; Qian, G.; Lobkovsky, E. B. *Adv. Mater.* **2007**, *19*, 1693–1696.
(8) Anjian, L.; Kunhao, L.; Haohan, W.; David, H. O.; Thomas, J. E.; Woosoek, K.; Maochun, H.; Jing, L. *Angew. Chem., Int. Ed.* **2009**, *48*, 2334–2338.
(9) Lan, A. J.; Li, K. H.; Wu, H. H.; Kong, L. Z.; Nijem, N.; Olson, D. H.; Emge, T. J.; Chabal, Y. J.; Langreth, D. C.; Hong, M. C.; Li, J. *Inorg. Chem.* **2009**, *48*, 7165–7173.
(10) Lan, A.; Li, K.; Wu, H. H.; Olson, D. J.; Emge, T.; Ki, W.; Hong, M.; Li, J. *Angew. Chem., Int. Ed.* **2009**, *48*, 2334–2338.
(11) Nakagawa, K.; Tanaka, D.; Horike, S.; Shimomura, S.; Higuchi, M.; Kitagawa, S. *Chem. Commun.* **2010**, *46*, 4258–4260.

10.1021/ja104923f

unsaturated metal center MOFs have been based on the determination of the adsorption sites via neutron scattering and loading via isotherm measurements.[33,34,41] Neutron diffraction is particularly useful to determine H_2 location for ordered H_2 incorporation (usually at saturation), and inelastic neutron scattering gives insight into rotational properties of H_2 in MOFs. Isotherm adsorption measurements give valuable information about hydrogen uptake and initial isosteric heats of adsorption of H_2 in MOFs. However, they do not provide direct information about adsorption sites and interaction potentials.

Infrared (IR) absorption measurements, on the other hand, are sensitive to interaction potentials and specific adsorption sites within the hosts and have been used to study incorporation of H_2 in solids.[42,43,44−47] Because the internal H−H stretch of free H_2 molecule is IR inactive, IR spectroscopy is only sensitive to H_2 molecules that interact with the host (or other molecules), that is, that undergo perturbation of the local H−H bonding. This perturbation is usually accompanied by a red shift of the H−H stretch modes, located at 4161.1 and 4155 cm^{-1} for free para and ortho H_2, respectively.[48−50] Traditionally, IR shifts of adsorbed H_2 have been correlated with their binding energies and the integrated areas for specific IR bands with the amount (loading) of adsorbed H_2.[42,43,51] These correlations have been based on the assumptions that (i) the dipole moment of adsorbed H_2 is not affected by loading or site geometry, and (ii) the largest H−H stretch is for H_2 adsorbed on unsaturated rather than saturated metal sites. In a recent IR spectroscopy study of MOFs with saturated metal centers performed at high pressures and room temperature, we have shown that the H−H stretch shift does not correlate to binding energies and is instead dominated by interactions with the ligands.[52] It is therefore important to examine the IR absorption spectra of H_2 in MOFs with unsaturated metal centers such as MOF-74.

MOF-74 (M_2(dhtp), dhtp = 2,5-dihydroxyterephthalate) consists of a three-dimensional honeycomb lattice with one-dimensional pores (diameter ∼12 Å). The benzenedicarboxylates ligands connect the metal centers via an oxygen atom. In the present study of MOF-74, a model system for MOFs with coordinatively unsaturated metal centers,[34,53−59] we find that H_2 adsorbed at the metal center (highest binding energy site) is characterized by an H_2 stretch shift of smaller magnitude (∼30 cm^{-1}) than that for H_2 in MOFs with saturated metal centers (∼38 cm^{-1}) when no other sites are occupied (low loading regime). Upon population of the next available site (the "oxygen" site), the magnitude of the H_2 stretch frequency shift is dramatically increased to a value (∼ −70 cm^{-1}) that is similar to what was previously observed by other groups studying unsaturated metal center systems including a recent study on MOF-74.[42−60] Theoretical calculations based on a van der Waals density functional (vdW-DF)[61−63] approach show that the increased shift is due to the interaction between H_2 molecules

(12) Li, Q.; Zhang, W.; Miljanic, O. S.; Sue, C.-H.; Zhao, Y.-L.; Liu, L.; Knobler, C. B.; Stoddart, J. F.; Yaghi, O. M. *Science* **2009**, *325*, 855–859.
(13) Ferey, G.; Mellot-Draznieks, C.; Serre, C.; Millange, F.; Dutour, J.; Surble, S.; Margiolaki, I. *Science* **2005**, *309*, 2040–2042.
(14) Klontzas, E.; Mavrandonakis, A.; Tylianakis, E.; Froudakis, G. E. *Nano Lett.* **2008**, *8*, 1572–1576.
(15) Li, J.-R.; Kuppler, R. J.; Zhou, H.-C. *Chem. Soc. Rev.* **2009**, *38*, 1477–1504.
(16) Xiao, B.; Yuan, Q. *Particuology* **2009**, *7*, 129–140.
(17) Zacher, D.; Shekhah, O.; Woll, C.; Fischer, R. A. *Chem. Soc. Rev.* **2009**, *38*, 1418–1429.
(18) Kurmoo, M. *Chem. Soc. Rev.* **2009**, *38*, 1353–1379.
(19) Rosseinsky, M. J. *Nat. Mater.* **2010**, *9*, 609–610.
(20) Ma, L.; Falkowski, J. M.; Abney, C.; Lin, W. *Nat. Chem.* **2010**, *2*, 838−846.
(21) Corma, A.; Garcia, H.; Llabres i Xamena, F. X. *Chem. Rev.* **2010**, *110*, 4606–4655.
(22) Eddaoudi, M.; Kim, J.; Rosi, N.; Vodak, D.; Wachter, J.; O'Keefe, M.; Yaghi, O. M. *Science* **2002**, *295*, 469–472.
(23) Rosi, N. L.; Eddaoudi, M.; Kim, J.; O'Keeffe, M.; Yaghi, O. M. *CrystEngComm* **2002**, 401–404.
(24) Chae, H. K.; Kim, J.; Friedrichs, O. D.; O'Keefe, M.; Yaghi, O. M. *Angew. Chem., Int. Ed.* **2003**, *42*, 3907–3909.
(25) Satyapal, S.; Petrovic, J.; Read, C.; Thomas, G.; Ordaz, G. *Catal. Today* **2007**, *120*, 246–256.
(26) Yu-Fei, S.; Leroy, C. *Angew. Chem., Int. Ed.* **2008**, *47*, 4635–4637.
(27) Proch, S.; Herrmannsdörfer, J.; Kempe, R.; Kern, C.; Jess, A.; Seyfarth, L.; Senker, J. *Chem.-Eur. J.* **2008**, *14*, 8204–8212.
(28) Liu, Y.-Y.; Zeng, J.-L.; Zhang, J.; Xu, F.; Sun, L.-X. *Int. J. Hydrogen Energy* **2007**, *32*, 4005–4010.
(29) Mulfort, K. L.; Hupp, J. T. *J. Am. Chem. Soc.* **2007**, *129*, 9604–9605.
(30) Mulfort, K. L.; Farha, O. K.; Stern, C. L.; Sarjeant, A. A.; Hupp, J. T. *J. Am. Chem. Soc.* **2009**, *131*, 3866–3868.
(31) Nouar, F.; Eckert, J.; Eubank, J. F.; Forster, P.; Eddaoudi, M. *J. Am. Chem. Soc.* **2009**, *131*, 2864–2870.
(32) Wang, L.; Yang, R. T. *Energy Environ. Sci.* **2008**, *1*, 268–279.
(33) Liu, Y.; Kabbour, H.; Brown, C. M.; Neumann, D. A.; Ahn, C. C. *Langmuir* **2008**, *24*, 4772–4777.
(34) Zhou, W.; Wu, H.; Yildirim, T. *J. Am. Chem. Soc.* **2008**, *130*, 15268–15269.
(35) Thomas, K. M. *Dalton Trans.* **2009**, 1487–1505.
(36) Rowsell, J. L. C.; Yaghi, O. M. *J. Am. Chem. Soc.* **2006**, *128*, 1304–1315.
(37) Dincă, M.; Long, J. *Angew. Chem., Int. Ed.* **2008**, *47*, 6766–6779.
(38) Britt, D.; Furukawa, H.; Wang, B.; Glover, T. G.; Yaghi, O. M. *Proc. Natl. Acad. Sci. U.S.A.* **2009**, *106*, 20637–20640.
(39) Dincă, M.; Dailly, A.; Liu, Y.; Brown, C. M.; Neumann, D. A.; Long, J. R. *J. Am. Chem. Soc.* **2006**, *128*, 16876–16883.
(40) Rosi, N. L.; Kim, J.; Eddaoudi, M.; Chen, B.; O'Keeffe, M.; Yaghi, O. M. *J. Am. Chem. Soc.* **2005**, *127*, 1504–1518.
(41) Brown, C. M.; Liu, Y.; Yildirim, T.; Peterson, V. K.; Kepert, C. *Nanotechnology* **2009**, *20*, 204025.
(42) Bordiga, S.; Regli, L.; Bonino, F.; Groppo, E.; Lamberti, C.; Xiao, B.; Wheatley, P. S.; Morris, R. E.; Zecchina, A. *Phys. Chem. Chem. Phys.* **2007**, *9*, 2676–2685.
(43) Vitillo, J. G.; Regli, L.; Chavan, S.; Ricchiardi, G.; Spoto, G.; Dietzel, P. D. C.; Bordiga, S.; Zecchina, A. *J. Am. Chem. Soc.* **2008**, *130*, 8386–8396.
(44) Gribov, E. N.; Bertarione, S.; Scarano, D.; Lamberti, C.; Spoto, G.; Zecchina, A. *J. Phys. Chem. B* **2004**, *108*, 16174–16186.
(45) Chabal, Y. J.; Patel, C. K. N. *Rev. Mod. Phys.* **1987**, *59*, 835.
(46) FitzGerald, S. A.; Allen, K.; Landerman, P.; Hopkins, J.; Matters, J.; Myers, R.; Rowsell, J. L. C. *Phys. Rev. B* **2008**, *77*, 224301.
(47) FitzGerald, S. A.; Churchill, H. O. H.; Korngut, P. M.; Simmons, C. B.; Strangas, Y. E. *Phys. Rev. B* **2006**, *73*, 155409.
(48) Welsh, H. L. *J. Atmos. Sci* **1969**, *26*, 835–840.
(49) Spoto, G.; Vitillo, J. G.; Cocina, D.; Damin, A.; Bonino, F.; Zecchina, A. *Phys. Chem. Chem. Phys.* **2007**, *9*, 4992–4999.
(50) Herzberg, G. *Molecular Spectra and Molecular Structure, Spectra of Diatomic Molecules*; van Nostrand: Princeton, NJ, 1989; Vol. 1.
(51) Garrone, E.; Arean, C. O. *Chem. Soc. Rev.* **2005**, *34*, 846–857.
(52) Nijem, N.; Veyan, J.-F.; Kong, L.; Li, K.; Pramanik, S.; Zhao, Y.; Li, J.; Langreth, D.; Chabal, Y. J. *J. Am. Chem. Soc.* **2010**, *132*, 1654–1664.
(53) Dietzel, P. D. C.; Blom, R.; Fjellvåg, H. *Eur. J. Inorg. Chem.* **2008**, 3624–3632.
(54) Bonino, F.; Chavan, S.; Vitillo, J. G.; Groppo, E.; Agostini, G.; Lamberti, C.; Dietzel, P. D. C.; Prestipino, C.; Bordiga, S. *Chem. Mater.* **2008**, *20*, 4957–4968.
(55) Dietzel, P. D. C.; Johnsen, R.; Blom, R.; Fjellvåg, H. *Chem.-Eur. J.* **2008**, *14*, 2389–2397.
(56) Dietzel, P. D. C.; Panella, B.; Hirscher, M.; Blom, R.; Fjellvag, H. *Chem. Commun.* **2006**, 959–961.
(57) Caskey, S. R.; Wong-Foy, A. G.; Matzger, A. J. *J. Am. Chem. Soc.* **2008**, *130*, 10870–10871.
(58) Millward, A. R.; Yaghi, O. M. *J. Am. Chem. Soc.* **2005**, *127*, 17998–17999.
(59) Dietzel, P. D. C.; Morita, Y.; Blom, R.; Fjellvåg, H. *Angew. Chem., Int. Ed.* **2005**, *44*, 6354–6358.
(60) FitzGerald, S. A.; Hopkins, J.; Burkholder, B.; Friedman, M.; Rowsell, J. L. C. *Phys. Rev. B* **2010**, *81*, 104305.
(61) Dion, M.; Rydberg, H.; Schroder, E.; Langreth, D. C.; Lundqvist, B. I. *Phys. Rev. Lett.* **2004**, *92*, 246401.
(62) Guillermo, R.-P.; Jose, M. S. *Phys. Rev. Lett.* **2009**, *103*, 096102.

located at the metal and oxygen sites. The calculations and experimental findings at higher loading also indicate that large variations in induced dipole moments for H_2 molecules take place as a function of loading.

2. Background on MOF-74 Studies

2.1. MOF-74. With its high density of coordinatively unsaturated metal centers, the class of MOF-74 materials features the largest surface density of adsorbed H_2 at 77 K.[33] Four adsorption sites have been identified by neutron scattering for H_2 in MOF-74:[33] the primary adsorption site near the unsaturated metal center, a secondary site near the triangle of oxygen atoms, a third near the benzene ring, and a fourth in the central region of the 1-D pore.[33] Furthermore, the relative orientation of the two H_2 molecules located near the primary (metal) and secondary (oxygen) sites has been theoretically determined.[64] Interestingly, the isosteric heats of adsorption appear to increase initially with coverage at low coverages to reach a value of 8.3 kJ/mol, suggesting that there may be effects due to H_2-H_2 interactions.[33,36] Moreover, a neutron scattering and a theoretical study have shown that the D_2-D_2 distance is as short as ~2.85 Å at 4 K between the zinc and oxygen sites in MOF-74-Zn, suggesting that H_2 loading can be increased thanks to the presence of the unsaturated Zn^{2+} centers.[33,64] However, many of the conclusions derived from isosteric heats of adsorption are indirect. On the other hand, theoretical interpretation[64] of inelastic neutron scattering data[33] suggests that the rotational spectrum of H_2 at the metal (Zn) site is dependent on whether or not the neighboring oxygen site is occupied, thus providing a precursor to the interaction effect described in this Article.

2.2. Vibrational and Theoretical Studies. H_2-H_2 interactions resulting from the proximity of adsorption sites are expected to cause dramatic changes in the H_2 stretch frequency of molecules located at the primary site when the secondary "oxygen" site is occupied. Such effects can be observable by IR spectroscopy that is directly sensitive to H_2-H_2 interactions at all loading conditions. A comprehensive study over a range of H_2 loadings and temperatures is necessary to uncover the nature of these interactions. Recently, an IR study was performed using diffuse reflectance spectroscopy, focusing on a narrow temperature range (~40 K).[60] In this work, vibrational and rotovibrational IR bands were observed, and a traditional analysis was performed on the basis of the assumption that the H−H stretch frequency scales with adsorption energy. While this work acknowledged the unusual isosteric heat of adsorption behavior observed by others,[33,36] the standard assignment of the IR modes was not consistent with the complex behavior of this system. In particular, the assignment of a weak (~ -2 cm^{-1}) shift to H_2-H_2 interactions was not substantiated, highlighting the fundamental shortcomings of such analysis.

In the present study, we have characterized the interaction of hydrogen with unsaturated metal center MOF-74-M (M = Zn, Mg, Ni) (M_2(dhtp), dhtp = 2,5-dihydroxyterephthalate) having hexagonal 1-D pore structures; the M^{+2} cations are bonded to five oxygen atoms in a square-pyramid coordination (see Figure S1 in the Supporting Information).[36,40,53,56,59] We provide both experimental and theoretical evidence for H_2-H_2 interactions in MOF-74 systems with different metal centers, manifested most clearly as large variations in H_2 IR shifts and dipole moments. The novelty of this work is the combination of high-pressure, room temperature measurements and lower-pressure, low temperature measurements over a large temperature range (15−100 K) with vdW-DF calculations that can treat H_2 interactions in large unit cells.[64,65] This combination is critical to show that the H−H stretch dipole moment strongly depends on loading and that the H−H stretch frequency shifts are more strongly affected by H_2-H_2 interactions than by binding energies, which had not been recognized before.

First-principles calculations based on density-functional theory have been applied to H_2 adsorption in these systems. In general, the GGA underestimates while LDA overestimates the binding energy significantly. For example, the GGA gives a static binding energy of 4.43 kJ/mol and LDA gives 21.97 kJ/mol for MOF-74-Zn,[34] while the measured Q_{st} is ~8.8 kJ/mol.[33,36] The zero point energy (ZPE) correction (typically around 2−3 kJ/mol[64]) brings the LDA values slightly closer to experimental results, but makes the GGA results even worse. Density functional calculations have also been applied to another MOF structure with unsaturated metal centers, HKUST-1, where the GGA results give a surprisingly high binding energy of ~31 kJ/mol[41] in contrast to a much lower experimental Q_{st} (~7 kJ/mol[36]). The LDA is even worse with ~52 kJ/mol. These results demonstrate the inadequacy of the ordinary DFT to describe the H_2-MOF interactions, even for systems with unsaturated metal centers, in which electrostatic interactions are expected to play an important role.

The vdW-DF theoretical approach has been applied to H_2 adsorption in several MOF systems and is very useful in locating adsorption sites and obtaining approximate stretch frequency shifts of adsorbed H_2.[52,65] An effective binding energy of ~10 kJ/mol after ZPE correction was obtained for H_2 in MOF-74-Zn in much better agreement with Q_{st} than the GGA or LDA results.[64] Here, we further extend this approach to calculate the transition dipole moment associated with H_2 stretching vibrations using the maximally localized-Wannier-function scheme.[66−69] The calculated dynamic dipole moment allows us to access the integrated IR intensity, which is proportional to the square of the dipole moment, thereby supplementing the information that can be obtained from the energy positions of the IR peaks.

3. Materials and Methods

3.1. Material Synthesis.[34,40,55,57,59]

MOF74-Zn. 2,5-Dihydroxyterephthalic acid (99 mg, 0.5 mmol) and $[Zn(NO_3)_2]\cdot 6H_2O$ (298 mg, 1.0 mmol) were dissolved in THF (7 mL), NaOH solution (2 mL, 1 M), and water (3 mL) with stirring. The mixture was then sealed in a Teflon-lined autoclave and heated in an oven at 110 °C for 3 days. The product was collected by filtration as a light-yellow substance. Yield: 160 mg, 87%.

MOF74-Mg. MOF74-Mg was synthesized from 2,5-dihydroxyterephthalic acid (99 mg, 0.5 mmol) and $Mg(NO_3)_2\cdot 6H_2O$ (257 mg, 1.0 mmol) following the same procedure as in the synthesis of MOF74-Zn. Yield: 115 mg, 83%.

MOF74-Co. 2,5-Dihydroxyterephthalic acid (150 mg, 0.75 mmol) and $[Co(NO_3)_2]\cdot 6H_2O$ (186 mg, 0.75 mmol) were dissolved in 15 mL of THF−H_2O solution (v:v = 1:1) with stirring. The mixture was transferred to a Teflon-lined autoclave, which was then

(63) Thonhauser, T.; Cooper, V. R.; Li, S.; Puzder, A.; Hyldgaard, P.; Langreth, D. C. *Phys. Rev. B* **2007**, *76*, 125112.
(64) Kong, L.; Román-Pérez, G.; Soler, J. M.; Langreth, D. C. *Phys. Rev. Lett.* **2009**, *103*, 096103.
(65) Kong, L.; Cooper, V. R.; Nijem, N.; Li, K.; Li, J.; Chabal, Y. J.; Langreth, D. C. *Phys. Rev. B* **2009**, *79*, 081407−4.
(66) King-Smith, R. D.; Vanderbilt, D. *Phys. Rev. B* **1993**, *47*, 1651.
(67) Vanderbilt, D.; King-Smith, R. D. *Phys. Rev. B* **1993**, *48*, 4442.
(68) Marzari, N.; Vanderbilt, D. *Phys. Rev. B* **1997**, *56*, 12847.
(69) Souza, I.; Marzari, N.; Vanderbilt, D. *Phys. Rev. B* **2001**, *65*, 035109.

sealed and heated in an oven at 110 °C for 3 days. Brown-red rod-shape crystals were isolated after filtering and dried under vacuum. Yield: 130 mg, 50%.

MOF74-Ni. A mixture of 2,5-dihydroxyterephthalic acid (60 mg, 0.3 mmol), $[Ni(NO_3)_2]\cdot 6H_2O$ (174 mg, 0.6 mmol), DMF (9 mL), and H_2O (1 mL) was transferred to a Teflon-lined autoclave and heated in an oven at 100 °C for 3 days. Brown crystalline powder was collected after filtering and dried under vacuum. Yield: 75 mg, 72%.

3.2. Methods: Activation Procedure. The phase purity and crystallinity for the MOF samples was determined by powder X-ray diffraction (PXRD). The data are provided in Figure S10 in the Supporting Information. All as-synthesized materials were exchanged with fresh methanol four times in 4 days, dried in a vacuum at room temperature, and then annealed overnight in a vacuum (at ~480 K). The thermogravimetric analysis (TGA) provided in Figures S11−S13 in the Supporting Information indicates that all solvent-exchanged MOF-74 samples have high thermal stability. The guest-free samples can be easily obtained upon the removal of the methanol molecules by heating over 100 °C. MOF-74-Zn keeps its crystallinity until it is decomposed above 400 °C. For MOF-74-Mg, the decomposition temperature of the guest-free sample is also over 400 °C. However, for MOF-74-Mg upon the removal of solvent molecules, the curve reaches a long plateau, and the decomposition temperature is over 450 °C. MOF-74-Ni is less stable, and the decomposition of the guest-free framework occurs at ca. 350 °C. The PXRD analysis indicates that the whole MOF-74 series remain highly crystalline upon removal of solvent molecules.

A recent study has shown that the surface area and pore size can vary with the details of the pretreatment of the samples.[53] Our study also shows that hydrogen loading (integrated areas of a specific peak at the exact same conditions) depends somewhat on the activation procedure, heating time, and other pretreatment parameters.

3.3. IR Spectroscopy of H_2 Adsorption. Infrared absorption spectroscopy measurements were first performed in transmission at room temperature using a liquid N_2 cooled indium antimonide detector. A portion (~10 mg) of the activated MOF was lightly pressed onto a KBr support and mounted into a high temperature, high pressure cell (Specac product number P/N 5850c) and further heated in vacuum. Hydrogen gas was introduced into the cell at various pressures (20−41 kTorr), using deuterium gas as a reference for hydrogen absorption spectra to remove perturbation of the MOFs vibrational spectrum due to high pressure gas loading. The same sample was then loaded into a Janis PTSHI series cold refrigerator (CCR) system, and the sample was heated overnight to 480 K in a vacuum to remove adsorbed water that strongly adsorbs into MOFs with unsaturated metal centers. Measurements were performed in transmission using a liquid N_2 cooled indium antimonide detector, in the pressure range 0.04−1000 Torr and in the temperature range 298−20 K.

At room temperature and high pressures of 20−41 kTorr (27−55 bar), homonuclear diatomic molecules such as hydrogen become detectable by IR spectroscopy because the electronic distribution is perturbed by collisions.[48] This collision-induced IR absorption scales as the square of the pressure[48,70] and must be removed from the final absorption spectra. Therefore, pure hydrogen gas IR absorption spectra are measured in the absence of MOF material at all relevant pressures and subtracted from the absorption spectra recorded with the MOF material at similar pressures.[52] Variations in IR absorption intensities are observed in different samples due to the method of activation, thermal cycling, and sample preparation. Furthermore, pressing the powder sample onto KBr pellets can lead to differences of H_2 incorporation at low temperatures due to the limited ability of H_2 to penetrate into the interior part of the sample. However, for a specific sample in a given run, the intensities are reproducible, and their functional dependence on pressure and temperature is identical.

3.4. Theoretical Methods. First-principles calculations based on van der Waals density functional theory were performed within the plane-wave implementation of the density functional theory in the ABINIT package,[71,72] which we have adapted from the Siesta[73,74] code to incorporate the van der Waals interaction. We used Troullier−Martins pseudopotentials[75] with a gradient-corrected functional. An energy cutoff of 50 Ry and Gamma point sampling were found to be enough to obtain the interaction energy converged to within 0.1 kJ/mol and the frequency shift within 1 cm^{-1}. The experimental structures of MOF-74-Zn were taken from Liu et al.[33] For MOF-74-Mg, we used the lattice constant from Zhou et al.[34] and relaxed the MOF atoms with generalized-gradient approximation (GGA). The MOF structures obtained were kept fixed upon H_2 adsorption and bond stretching for both Zn and Mg cases.

To obtain the H_2 adsorption sites, we performed self-consistent vdW-DF energy minimizations in which the H atoms are allowed to relax. Once these equilibrium positions were established, we then carried out a series of total energy calculations with different H_2 bond lengths while keeping the center of H_2 and the MOF atoms at their equilibrium positions. The resulting total energies were used in the Schrodinger equation to obtain the eigenvalues, and the difference of the two lowest eigen levels gives the vibrational frequency. The H_2 adsorption potential is anharmonic, and it is important to include anharmonicity in the calculation. The approach we use fully does not use a harmonic approximation and is thus well suited for dealing with such systems. For the case of the more strongly interacting H_2-H_2 pair at the metal and O sites, the above method was successfully tested using the normal coordinates of the H_2-H_2 pair. We note that the H_2 orientation in our frequency calculation is "frozen" at its equilibrium value, while the real H_2 behaves as a hindered rotor in the MOF.[41] The orientational delocalization in general leads to ro-vibrational coupling. For free H_2, the coupling is proportional to $\alpha_e(v + 1/2)J(J + 1)$, where v and J are the vibrational and rotational quantum numbers, and α_e is the coupling constant (~3 cm^{-1} for free H_2). To get the coupling effect for H_2 inside MOF requires solving the full Schrodinger equation for the adsorbed H_2 with six-dimensional potential energy surface, which is beyond the current computational capabilities. We expect a similar coupling effect for the adsorbed H_2 as for the free H_2 because the H_2-MOF interaction is quite weak and serves as a small perturbation to the H_2 stretch motion. Furthermore, we calculate the stretch frequency for both adsorbed and free H_2 and compare the shift. The error of neglecting the coupling exists for both cases and should somewhat cancel each other, minimizing the ro-vibrational coupling effect in the frequency shift.

The dipole moment is estimated from maximally localized-Wannier-function method.[66,67] In this approach, the continuous electron density can be replaced with a point charge located at the Wannier center based on the Berry-phase theory of polarization.[68,69] The dipole moment per cell is then given by

$$\mu = e\sum_i Z_i R_i - 2e\sum_n r_n \qquad (1)$$

where Z_i and R_i are the atomic number and position of the ith nucleus in the unit cell, and r_n is the position of the nth Wannier center. The factor of 2 before the second summation accounts for the spin degeneracy. The quantity e is the magnitude of the

(70) Frommhold, L. *Collision-Induced Absorption in Gases*; Cambridge University Press: New York, 1993.

(71) Gonze, X.; et al. *Comput. Mater. Sci.* **2002**, *25*, 478–492.
(72) Gonze, X.; et al. *Z. Kristallogr.* **2005**, *220*, 558–562.
(73) Soler, J. M.; Artacho, E.; Gale, J. D.; Garcia, A.; Junquera, J.; Ordejon, P.; Sanchez-Portal, D. *J. Phys.: Condens. Matter* **2002**, *14*, 2745–2779.
(74) Ordejón, P.; Artacho, E.; Soler, J. M. *Phys. Rev. B* **1996**, *53*, R10441.
(75) Troullier, N.; Martins, J. L. *Phys. Rev. B* **1991**, *43*, 1993.

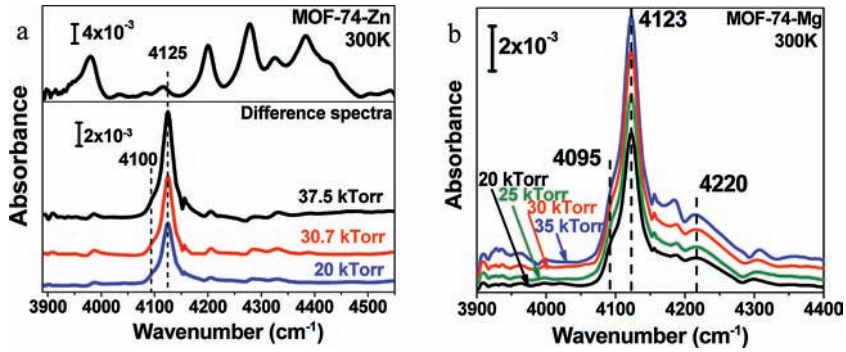

Figure 1. (a) IR absorption spectra at 300 K of (top) activated MOF74-Zn referenced to KBr in a vacuum and (bottom) the difference spectra of hydrogen and deuterium showing $\Delta\nu$(H−H) of −30 cm^{-1}; and (b) IR absorption spectra of H_2 adsorbed in MOF-74-Mg. Small features are due to perturbation of the MOF structure, when subtraction from deuterium is not performed.

electronic charge. To a good approximation, the dipole moment varies linearly with the H_2 vibrating normal coordinates Q, as

$$\mu(Q) = \mu_0 + \frac{d\mu}{dQ}Q \qquad (2)$$

where μ_0 is the dipole moment in the equilibrium position. $d\mu/dQ$ has the unit of charge and is often called effective charge, e^*, which is proportional to the dynamic dipole moment that is induced by the IR electric field. Because the absorption coefficient is proportional to the square of the matrix element of this dynamic dipole moment between the initial and final state, it is therefore proportional to the square of the effective charge.

The Wannier functions were calculated with the Wannier90 code[76] embedded in ABINIT,[71,72] and the Brillouin zone was sampled by a 2 × 2 × 2 Monkhorst−Pack grid. We used the H_2 internuclear distance as an approximation for the stretching normal coordinates and calculated the effective charge by taking the difference between the dipole moments at two different bond lengths. To reduce the numerical errors, the bond stretching should be sufficiently large, but still in the linear regime. We found that a stretch of 0.05 A from equilibrium bond length was appropriate. Further details of the dipole moment calculation will be given in a forthcoming paper.

4. Results

4.1. Low Loading Studies To Identify Isolated H_2 Adsorbed at the Metal Site. Room temperature studies of H_2 adsorbed in MOFs are important to ensure that only the higher binding energy sites are occupied. In a large pressure range (750 Torr to 45 kTorr), the concentration of H_2 is very low (typically ∼1 H_2 per unit cell, i.e., <10% of saturation loading) in most MOFs. Moreover, the temperature is high enough to overcome any activation or diffusion barrier necessary to occupy this or other sites. Therefore, in such studies of MOF-74, the highest binding energy site (i.e., the metal site) is guaranteed to be occupied uniformly within the microcrystals. It is possible for the secondary adsorption sites (near the oxygen in this case) to be partially occupied at room temperature, given their heat of adsorption ($Q_{st} \approx 5$ kJ/mol), assuming a Boltzmann distribution and a uniform occupation.

At very low temperatures (i.e., 15 K or below), the situation is typically much more complicated because H_2 incorporation into the MOF is severely limited by diffusion and in some cases by the inability to populate some sites due to kinetic barriers. As a result, only the periphery of the MOF-74 crystallites can be occupied, more spatial inhomogeneity results, and only sites without kinetic barriers are accessible. Occupation of other sites that require some activation is not possible at these low temperatures.

In view of these considerations, IR absorption measurements of hydrogen interaction with unsaturated metal center MOF-74-M (M = Zn, Ni, Mg) were first performed at room temperature and high pressures (20−41 kTorr) to study H_2 at the metal site, and then at 15 K to investigate kinetic barriers.

Room Temperature Data. The spectra in Figure 1 reveal that, at room temperature and high pressures, the H−H stretch vibration displays a remarkably small shift (∼ −30 cm^{-1}) from the value of the unperturbed *ortho*-H_2 at 4155 cm^{-1} for both MOF-74-Zn and MOF-74-Mg. As previously discussed, there is some infrared absorption in the H−H stretch spectral region (3900−4500 cm^{-1}) arising from overtone and combination bands of the MOF itself.[52] The top part of Figure 1a shows the spectrum associated with combination and overtone absorption bands of MOF-74-Zn, measured in a vacuum, and referenced to a MOF-free supporting KBr pellet in vacuum. The bottom part of Figure 1a shows IR absorption of adsorbed H_2 obtained by subtracting the spectrum of D_2 at the same pressure. The spectrum of the H_2 gas phase in that region (in the cell outside the MOF) is subtracted by recording spectra without the MOF at similar pressures.[52] The subtraction of adsorbed hydrogen IR spectra from deuterium is necessary to reduce the features in the IR spectra caused by the perturbation of the MOF structure by the adsorbents, resulting in blue shifts of the overtone and combination bands, as illustrated by the features observed, for instance, in the case of MOF-74-Mg (Figure 1b).[52]

The spectra in Figure 1 are dominated by a main band for both MOF-74-Zn and MOF-74-Mg centered at ∼4125 cm^{-1} in the case of MOF-74-Zn and 4123 cm^{-1} in the case of the Mg metal center with a weak shoulder at ∼4100 cm^{-1}. On the basis of the arguments presented earlier and later supported by calculations, this band is assigned to ν(H−H) of isolated H_2 in close proximity to the metal center. The resulting shifts are −30, −32, and −34 cm^{-1} for Zn, Mg, and Ni metal centers, respectively (see Figure S2 in the Supporting Information). Clearly, the position of the H−H stretch frequency depends weakly on the three types of metal center, varying only by <4 cm^{-1} when the metal center is exchanged. All these shifts are substantially smaller than what was measured previously at ∼77 K for MOF-74-Ni.[43] Table 1 summarizes the data for Zn, Mg, and Ni metal centers and points to only a weak dependence on the metal center, potentially due to the columbic interaction that was also identified as the primary interaction in a previous

(76) Mostofi, A. A.; Yates, J. R.; Lee, Y.-S.; Souza, I.; Vanderbilt, D.; Marzari, N. *Comput. Phys. Commun.* **2008**, *178*, 685–699.

Table 1. Comparison between the Different Properties of MOF-74-M

unsaturated metal center	Q_{st}[34] [kJ/mol]	$d(M-H_2)$[34] [Å]	$\Delta\nu(H-H)$ [cm^{-1}]	$\nu(H-H)$ 300 K [cm^{-1}]	$\nu(H-H)$ 15 K [cm^{-1}]
Zn	8.5	2.83	−30	4125	4128−4134
Mg	10.1	2.54	−32	4123	4125−4134
Ni	12.9	2.00	−34	4121	NA

study.[34] The main finding is that the H_2 shift measured at 300 K is -30 cm^{-1} instead of ~ -70 cm^{-1} for MOF-74-Zn at 40 K and -34 cm^{-1} instead of ~ -120 cm^{-1} for MOF-74-Ni at low temperatures (T < 180 K) as was reported in earlier work.[43,60]

Figure 2 shows that the integrated intensities of the ν(H−H) IR absorption bands at room temperature for the different MOF-74-M increases linearly with pressure. This linear behavior confirms that this band is not due to H_2 gas (characterized by a quadratic dependence on pressure[48]), but to H_2 trapped in the pores. Isotherm measurements performed at similar conditions show that the occupation is <1 H_2/unit cell, confirming that the IR band at 4125 cm^{-1} corresponds to H_2 isolated on the metal site.[77] At this temperature, only the highest binding energy sites are occupied, the metal sites, because the loading is too low for occupation of the oxygen or other sites.

Low Temperature Data (15 K). The IR absorption measurements performed at low temperatures such as 15 K (Figure 3a,b) are complicated by many factors: (1) Kinetic limitations may prevent the uniform penetration of the macroscopic sample, (2) the occupation of other sites may be hindered by activation barriers that cannot be overcome at such low temperatures, and (3) H_2 liquefaction outside the sample may occur at such temperatures (liquid H_2 occurs at 20 K and 1 bar). The IR absorption spectra of adsorbed H_2 collected for MOF-74-Zn (Figure 3a) and MOF-74-Mg (see Figure S3 in the Supporting Information) at 15 K show that the IR absorption bands centered at 4129 cm^{-1} for the case of Zn metal center and 4135 cm^{-1} for the Mg metal center are again substantially less shifted (~ -32 and -26 cm^{-1} from the unperturbed para H_2 position at 4161 cm^{-1}) than what was previously reported.[43] The main finding at 15 K is that the dominant absorption band is similar to what was measured at 300 K, presumably associated with isolated H_2 located at the metal site.

A closer examination of Figure 3a indicates that, in addition to the strong band centered at 4129 cm^{-1}, there is a very weak band at ~4093 cm^{-1} that increases with pressure. This weak band is located at a position that is much closer to what was observed at 77 K by other groups for MOFs with unsaturated metal centers[42,43] and might be associated to the occupation of a different site in the MOF-74 unit cell. The relative intensity of this weak band was also found to slightly increase with time, as summarized in Figure 3b and highlighted in the inset for 18 Torr showing changes occurring over a period of ~2 h at a given pressure. The data collected at the beginning of the scan (initial data) are used as reference, thus highlighting changes occurring over time.

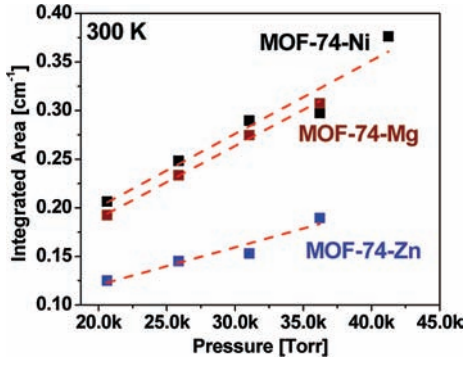

Figure 2. Integrated areas of hydrogen IR bands at 300 K for different MOF-74-M (M = Zn, Mg, and Ni) as a function of pressure, showing a linear dependence on pressure and an effect of the metal center.

These time-dependent measurements performed for a number of different H_2 pressures (Figure 3b) reveal that the IR absorption band centered at 4129 cm^{-1} shifts to 4143 cm^{-1} with time. There is also a decrease in intensity at 4129 cm^{-1}. The origin of this intensity decrease will be discussed in the following section. The +16 cm^{-1} shift is partially due to liquefaction of H_2 in the pores (~7 cm^{-1} blue shift) followed by ortho−para conversion (a 9 cm^{-1} blue shift for liquid H_2). Therefore, apart from ortho−para conversion and liquefaction, the main finding is that the 15 K data suggest that there is a configuration for adsorbed H_2 that leads to a substantially larger red shift (~ -70 cm^{-1}), similar to what was observed by another group at 40 K for MOF-74-Zn (~ -70 cm^{-1}), or for MOF-74-Ni (~ -120 cm^{-1}) and for HKUST (~ -70 cm^{-1}) using variable temperature IR studies.[42−60] The nature of the configuration giving rise to this larger shift will be described in the Discussion.

Figure 4 illustrates the main changes occurring with time in the two spectral features at 4129 and 4093 cm^{-1} in the spectra of Figure 3a. In contrast to Figure 3a that only shows changes in integrated areas (comparing initial and final areas as a function of pressure), Figure 4 shows the total intensities of the bands. Initially, only the band at 4129 cm^{-1} is observable, and its pressure dependence (black curve, Figure 4) is negligible. However, after 2 h, there is a clear loss of intensity at the lowest pressures (6 and 18 Torr). Above 30 Torr, there appears to be saturation. Correspondingly, the band at 4093 cm^{-1} appears weakly at 18 Torr and saturates at 30 Torr. Above 30 Torr, H_2 uptake is terminated due to kinetic limitations (inability for H_2 to diffuse deeper into the microcrystallite, past the unit cells that are already occupied within the periphery of the sample). These observations suggest that the formation of the H_2 configuration leading to absorption at 4093 cm^{-1} is kinetically limited and is correlated with the existence of isolated H_2 adsorbed at the metal site. This result is similar to calculations performed on MOF-74-Zn showing that the occupation of the oxygen site depends greatly on the occupation of the metal site.[64]

In view of the data presented above, it is not surprising that alternative loading protocols have been used in all previous work.[42,43] Specifically, loading was performed at 300 K and the sample was then slowly cooled to lower temperatures (e.g., 30, 40, and 77 K) to allow H_2 to fully diffuse throughout the sample. These procedures tend to achieve higher loadings, resulting in occupation of more than just the metal site. In the absence of corresponding isotherm measurements, these studies assumed that the initial IR absorption band detected at ~4090 cm^{-1} corresponded to H_2 at the metal center. The subsequent appearance of another band at higher frequency (i.e., smaller shift from the unperturbed H−H stretch frequency) was then attributed to the occupation of the oxygen site and the data used for variable temperature IR spectroscopy (VTIR) analysis to obtain adsorption enthalpies at specific sites.[43]

(77) Gallo, M.; Glossman-Mitnik, D. *J. Phys. Chem. C* **2009**, *113*, 6634–6642.

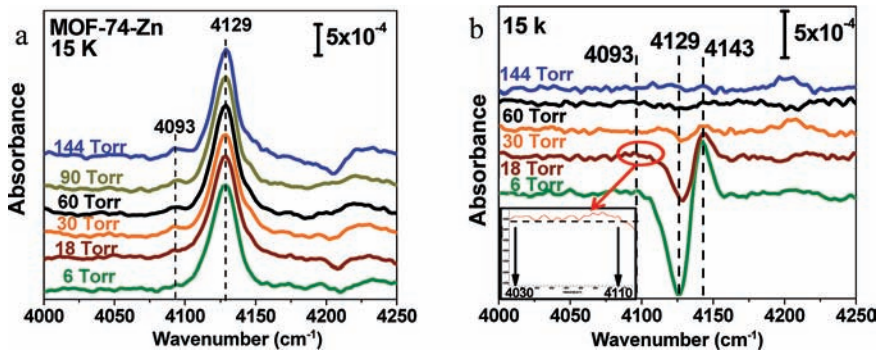

Figure 3. (a) IR absorption spectra of initial adsorption of hydrogen in MOF-74-Zn at 15 K as a function of pressure and (b) time-dependent IR spectra of adsorbed hydrogen at specific pressures over a 2 h period. The inset shows an increase at 4093 cm^{-1} at 18 Torr.

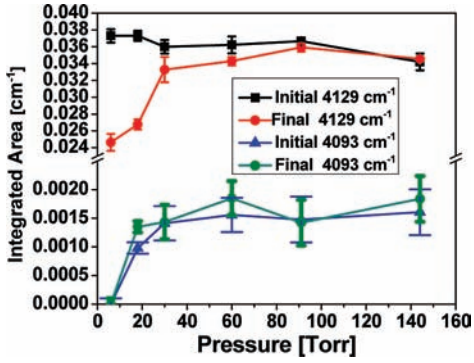

Figure 4. Integrated areas at 15 K of hydrogen IR bands at 4129 and 4093 cm^{-1}. Red and black curves represent initial and final (after 2 h) adsorption for the 4129 cm^{-1} IR band. Blue and green curves represent initial and final (after 2 h period) adsorption for the 4093 cm^{-1} IR band.

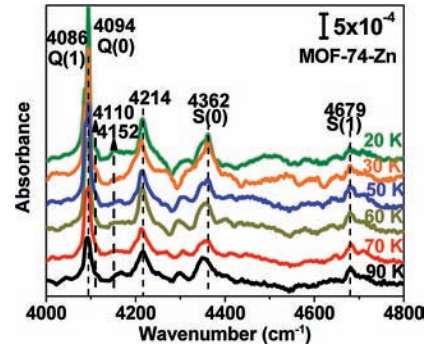

Figure 5. IR absorption spectra of adsorbed hydrogen in MOF-74-Zn as a function of temperature; initial hydrogen (20 Torr) was introduced at room temperature.

We will show in the next section that at these intermediate temperatures, both the metal and the oxygen sites are occupied and that there are dramatic changes in induced dipole moments that makes VTIR analyses impossible especially at low loading.

4.2. Infrared Absorption Measurements of Hydrogen at Higher and Intermediate Loading. The loading procedures used for this section are meant to reproduce the loading protocols used by other groups,[42,43,78] to understand the nature of H_2 giving rise to the mode at 4091 cm^{-1}.

Room Temperature Loading and Dependence on Temperature. For these experiments, 20 Torr hydrogen gas is introduced into the system at room temperature, containing MOF-74-Zn, and the system is then closed. IR absorption measurements are performed in situ as the temperature is lowered from 300 to 20 K. For temperatures above 120 K, no hydrogen can be detected because the loading is too low. The spectra presented in Figure 5 show data over the smaller range of temperatures (90−20 K) in which the bands are easily detected. Clearly, the spectrum is now dominated by an absorption band centered at 4091 cm^{-1}. Accompanying this band are other features corresponding to the translational state at 4214 cm^{-1} with rotational−vibrational bands $S(0)$ at 4362 cm^{-1} and $S(1)$ at 4679 cm^{-1}.

Loading at 77 K and Pressure Dependence. Loading MOF-74-M (M = Zn, Mg) with hydrogen at 77 K results in the appearance of sharp IR bands at 4093 and 4091 cm^{-1} (Figure 6) for MOF-74-Zn (a) and MOF-74-Mg (b), respectively, in the range 0.3−750 Torr (0.4−1000 mbar), which do not shift with pressure. These large IR shifts of ~ -70 cm^{-1} are in agreement with previous work performed under similar conditions for unsaturated metal center MOFs.[42,43] A band at 4127 cm^{-1} is also observed and intensifies with pressure. At low pressures (<120 Torr), this band is weak and observed at ~4122 cm^{-1} for MOF-74-Zn and at 4118 cm^{-1} for MOF-74-Mg, as shown in Figure S5 in the Supporting Information. This IR band was previously attributed to H_2 adsorbed on the secondary "oxygen" site.[60] Finally, translational modes are seen at 4210 and 4232 cm^{-1} for zinc and magnesium metal center MOF-74, respectively. The rotational−vibrational bands occur at $S(0) \approx$ 4380 cm^{-1} and $S(1) \approx$ 4610 cm^{-1} for Zn, and $S(0)$ at ~4347 cm^{-1} and $S(1)$ at 4595 cm^{-1} for Mg.

To help with interpretation of all the IR absorption features identified in Figure 6, isotherm measurements are performed on MOF-74-Mg at 77 K, as shown in Figure S4 (right) in Supporting Information. It is found that there is ~1.95 wt % of H_2 adsorbed at 750 Torr (1 bar), which is less than the approximate 3.6 wt % needed to completely occupy the three most strongly bound types of adsorption sites identified by Liu et al.[33] (the metal, oxygen, and benzene sites).

The intensity of the 4093 (4091) cm^{-1} mode for MOF-74-Zn(Mg) exhibits a similar pressure dependence for all MOF-74-M with a sharp increase at very low pressures and saturation thereafter. The integrated areas are larger for magnesium than for zinc, similar to what was observed for isotherm measurements performed at similar conditions and shown in Figure S4 (left) (Supporting Information) for MOF-74-Mg.[34]

Loading at 30 and 40 K and Pressure Dependence. Examining intermediate temperatures such as 30 and 40 K is important to understand the effect of loading on IR shifts and induced

(78) Bordiga, S.; Vitillo, J. G.; Ricchiardi, G.; Regli, L.; Cocina, D.; Zecchina, A.; Arstad, B.; Bjorgen, M.; Hafizovic, J.; Lillerud, K. P. *J. Phys. Chem. B* **2005**, *109*, 18237–18242.

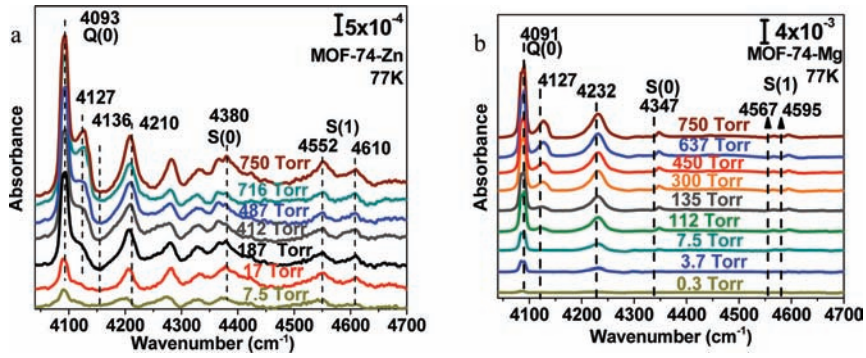

Figure 6. IR absorption spectra of adsorbed hydrogen for (a) MOF-74-Zn and (b) MOF-74-Mg at 77 K as a function of pressure. Gain translational states are observed $\sim +100$ cm^{-1} from the fundamental IR band of H_2 adsorbed on the metal site when the oxygen site is occupied. For the MOF-74-Zn case, deuterium gas at the same pressure was used to remove some bands that appear due to perturbation of the MOF structure.

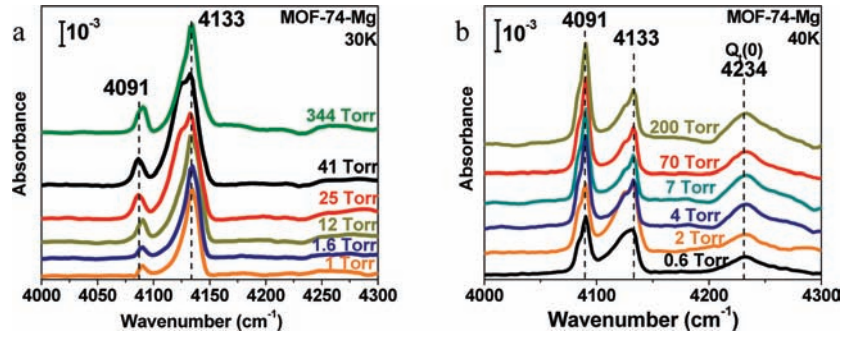

Figure 7. IR absorption spectra of final adsorption (after $\sim$2 h period) of hydrogen in MOF-74-Mg as a function of pressure (a) for a range of pressures 1−344 Torr at 30 K and (b) for 0.6−200 Torr at 40 K.

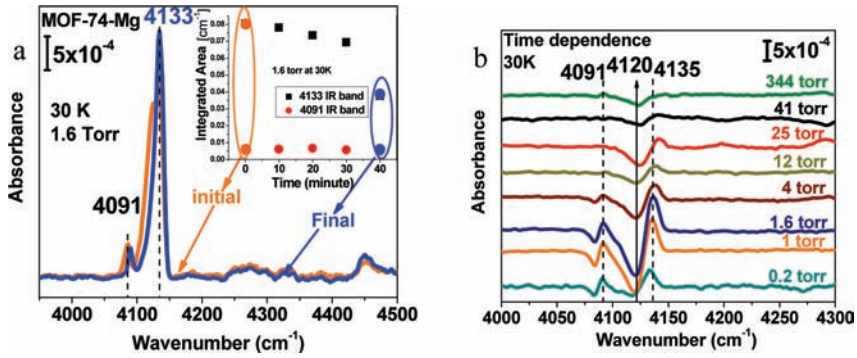

Figure 8. (a) Initial (orange) and final (blue) H_2 absorption spectra at 30 K and 1.6 Torr in MOF-74-Mg; inset shows the evolution of integrated areas of the IR bands at 4133 and 4091 cm^{-1} over a 40 min period. (b) Time-dependent IR spectra over $\sim$1 h period at specific pressures; final (end of 40 min) is referenced to initial. Note the colors of the IR time-dependent spectra match that of the IR absorption in Figure 7a.

dipole moments. For the current study, hydrogen is loaded at 30 and 40 K into MOF-74-Mg (previously activated by annealing to 480 K in vacuum $\sim$0.03 Torr), and spectra are recorded as a function of pressure. Figure 7a and b shows IR absorption spectra of H_2 adsorbed in MOF-74-Mg at 30 K (a) and 40 K (b) as a function of pressure from $\sim$1Torr (0.6 Torr at 40 K) to $\sim$345 Torr (200 Torr at 40 K). In an attempt to remove kinetic effects (described below), the measurements are carried out after a $\sim$2 h period for each pressure. At both temperatures two main IR bands are observed at 4091 and 4133 cm^{-1}, but their relative intensities depend strongly on temperature. The intensity of the band centered at 4091 cm^{-1} increases with pressure and is much higher at 40 than 30 K. The IR band centered at 4133 cm^{-1} has a relatively large fwhm of $\sim$32 cm^{-1}, which may be due to several components associated with different adsorption sites (see the Supporting Information and Figure S6). Furthermore, there is a band at 4234 cm^{-1} most visible at 40 K that follows that same pressure dependence as the band centered at 4091 cm^{-1}. This band is located $\sim$143 cm^{-1} higher than the fundamental IR absorption band and therefore associated with the frustrated translational motion of H_2. For completeness, a larger frequency range is presented in the Supporting Information in Figures S7 and S8, showing the rotational−vibrational bands $S(0)$ at $\sim$4448 cm^{-1} and $S(1)$ at $\sim$4700 cm^{-1}, which have recently been discussed in detail by FitzGerald et al.[60]

To investigate kinetic effects at these temperatures, time dependence studies were performed at both temperatures as a function of pressure. Figures 8a and 9a highlight the spectral evolution over a time of 40 min at 30 K and 1.6 Torr (Figure 8a) and 2 h at 40 K and 0.6 Torr (Figure 9a). The insets in these figures summarize the time dependence of the two main spectral contributions at 4091 cm^{-1} (red ●) and 4133 cm^{-1} (■). Clearly, equilibrium is reached at 40 K after $\sim$2 h, and not at

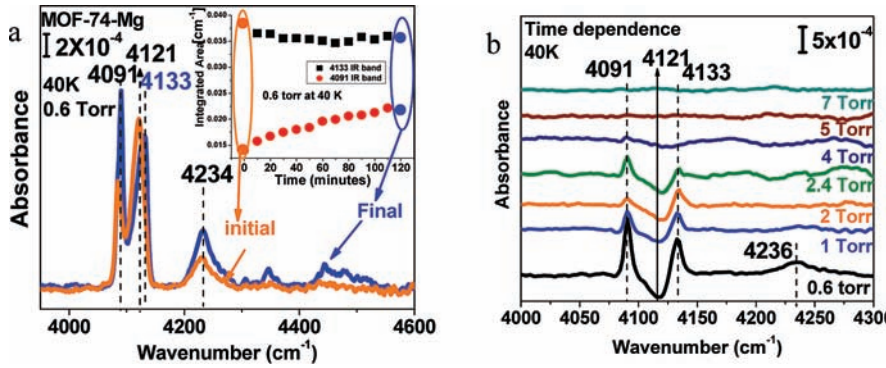

Figure 9. (a) Initial (orange) and final (blue) H_2 absorption spectra at 40 K and 0.6 Torr; inset shows the evolution of integrated areas of the IR bands at 4133 and 4091 cm^{-1} over a 2 h period. (b) Time-dependent IR spectra over ~2 h period at specific pressures; final (end of 2 h) is referenced to initial. Note the colors of the IR time-dependent spectra match that of the IR absorption in Figure 7b.

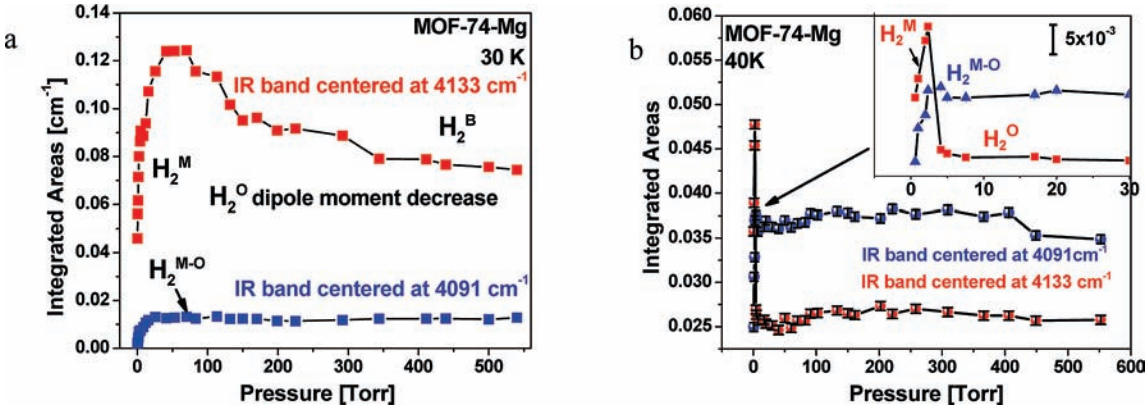

Figure 10. Integrated areas of the final (after 2 h period) IR bands centered at 4091 and 4133 cm^{-1} as a function of pressure for MOF-74-Mg at (a) 30 K and (b) 40 K. For both temperatures, a decrease in the IR band centered at 4133 cm^{-1} is observed. However, the intensity of this band is higher at 30 than 40 K. An increase in intensity of the IR band centered at 4091 cm^{-1} is observed for both cases at low pressures. H_2^M in the figures refers to H_2 adsorbed on the metal site, and H_2^{M-O} refers to H_2 adsorbed on the metal site when the oxygen site is occupied (H_2 pairing occur). The error in integrated areas taken by changing the baseline did not exceed 8×10^{-4} cm^{-1} in most cases.

30 K (equilibrium cannot be attained within reasonable times). For that reason, the time dependence of the integrated areas is only shown up to ~40 min, even though it does not correspond to equilibrium at 30 K.

Figures 8b and 9b show the spectral evolution over a period of 2 h for the spectra shown in Figure 7a (30 K) and b (40 K), using the same color coding. In these figures, the differential spectra are plotted using the spectra recorded within 10 min of establishing a given pressure as reference for the spectra collected after 2 h. These data show that the band at 4091 cm^{-1} increases with time in the lower pressure regime (0.2 to ~30 Torr at 30 K, and 0.6 to ~5 Torr at 40 K), while the band at ~4121 cm^{-1} weakens and blue shifts. The increase of the 4091 cm^{-1} mode is particularly significant for the lowest pressures at 40 K, although it is still less than 50% of the total intensity (see Figure 7b). One mechanism that leads to the blue shift of 4121 cm^{-1} band is ortho−para conversion, characterized by a ~6 cm^{-1} blue shift. However, the appearance and evolution of the 4135 (4133) cm^{-1} band could also involve population of other sites because as shown in Figure S6 (Supporting Information) this broad band constitutes many components. One component is H_2 adsorbed at the oxygen site at 4118 cm^{-1} also shown in Figure S5. The insets in Figures 8a and 9a show that the IR bands integrated areas are time dependent, which suggests that the loss of intensity of the band at 4121 cm^{-1} shown in Figure 8b results from more than just ortho−para conversion. Note that, in the differential spectra of Figures 8b and 9b, the frequencies marked at 4120 and 4135 or 4121 and 4133 cm^{-1} are not associated with modes at these exact frequencies because the changes are too close together. Instead, they indicate that the components of the broad band at 4133 cm^{-1} change (shift) in time. For instance, it is more likely that a component centered at 4125 cm^{-1} is lost (to reappear at 4091 cm^{-1}) and another around 4130 cm^{-1} appears.

Keeping in mind that 2 h is not sufficient to achieve equilibrium at 30 K but is sufficient at 40 K, the intensities of the two main bands at 4091 and 4133 cm^{-1} measured after 2 h (from Figure 7a and b) are plotted as a function of pressure in Figure 10 (a for 30 K and b for 40 K). The error bar of the integrated areas plotted in Figure 10 is less than 8×10^{-4} cm^{-1} and is due mostly to errors in baseline determination (i.e., integration). Focusing on the 40 K data in Figure 10b first, we note that the band centered at 4133 cm^{-1} initially increases up to ~3 Torr (i.e., as H_2 is loaded into the sample). However, there is a sharp integrated intensity drop from ~0.048 to ~0.025 cm^{-1} as the pressure is increased to ~5 Torr. Correspondingly, there is the appearance of the band at 4091 cm^{-1} with a sharp increase between 3 and 5 Torr. Note that the 4091 cm^{-1} band is more intense (integrated area ~0.036 cm^{-1}) than the 4133 cm^{-1} band (~ 0.026 cm^{-1}) after the transformation, indicating that these two bands are correlated at 40 K. Thereafter (>5 Torr), there is little change in either bands, presumably due to the fact that the interior part of the MOF microcrystallites might not be easily accessible due to slow kinetics (i.e., inability for H_2 to

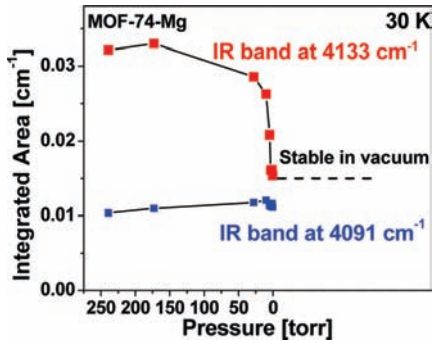

Figure 11. Integrated areas of IR bands at 4133 and 4091 cm^{-1} at 30 K for MOF-74-Mg as a function of pressure upon evacuation (error in evaluation of integrated areas did not exceed $\sim 5 \times 10^{-4}$ cm^{-1}).

diffuse deep inside the crystals) or the need for activation to occupy other sites.

At 30 K (Figure 10a), the situation is qualitatively similar with an increase of the 4133 and 4091 cm^{-1} bands at low pressures and little change in the latter past 20 Torr, but their magnitude and the pressure dependence of the 4133 cm^{-1} band are different. In contrast to the 40 K data (Figure 10a), the band at 4091 cm^{-1} is much weaker ($\sim$0.017 cm^{-1}), indicating that the occupation of the site leading to this band is minimal. The behavior of the broad band centered at 4133 cm^{-1} is complex. The initial increase at low pressures (<5 Torr) is consistent with isolated H_2 occupying metal sites as more H_2 is provided; that is, the pressure is increased. Yet the 4133 cm^{-1} band intensity increases higher than the peak obtained at 40 K (0.47 cm^{-1}) and decreases much more slowly as a function of pressure than at 40 K. The maximum integrated intensity is $\sim$0.125 cm^{-1} and the value at 500 Torr is $\sim$0.075 cm^{-1}, higher than the 0.027 cm^{-1} seen for 40 K. These observations are consistent with a relatively higher concentration of isolated H_2 at metal sites than at 40 K. In addition, they suggest that there are other contributions to the band at 4133 cm^{-1} that do not exist at 40 K. Indeed, neutron scattering data have shown that the first three adsorption sites can be fully occupied at 30 K. This indicates that the benzene site is most likely occupied under these conditions.[33] In all these measurements, the absolute integrated intensities are found to be sensitive to the activation procedures[53] and to the history of thermal cycling. The data for Figure 10 were obtained within one series of measurements on the same sample so that the intensities are comparable. However, repeated annealing cycles between series of measurements eventually led to lower intensities. Similarly, data taken on a different sample cannot be quantitatively compared because the activation is not identical (as noted for Figure 11 for instance). Keeping all these factors in mind, the main finding at 30 K is that the band at 4133 cm^{-1} is composed of several contributions, including the occupation of sites other than the metal and oxygen sites, such as the benzene sites, which are much more weakly bound.

If H_2 is able to occupy a lower binding energy site at 30 K (and not at 40 K) as suggested by Figure 10, the occupation of this site may be pressure dependent over some temperature range. We have therefore examined on a different sample in a one-time experiment the dependence of the 4133 cm^{-1} band as a function of pressure after loading the sample at 30 K and 250 Torr. Figure 11 shows that a portion ($\sim$1/2) of the total integrated intensity of the 4133 cm^{-1} band decreases as the pressure is lowered, particularly as a vacuum below 40 mTorr is established. The other half of the intensity remains stable under vacuum. As mentioned above, the absolute intensities are lower in this series of measurements than for Figure 10 because they are performed on another sample (slight differences in activation and thermal cycling history). For instance, the H_2 intensity achieved by loading at 250 Torr at 30 K ($\sim$0.2 cm^{-1}) is about $\sim$1/3 of what is reported in Figure 10a. Despite these differences, the dependence on pressure is fully reproducible. Figure 11 shows that one component contributing to the 4133 cm^{-1} band is strongly pressure dependent at 30 K, while the other half is not, similar to the band at 4091 cm^{-1}.

In summary, room temperature (high pressures) and 15 K (low pressures) experiments show clearly that shifts corresponding to isolated H_2 adsorbed at the metal site are less (~ -30 cm^{-1}) than what was previously assigned by others.[42−60] Experiments involving loading at room temperature and then cooling or at 77 K lead to the appearance of the IR band with larger red shift (~ -70 cm^{-1}) similar to previously observed shifts.[42−60] Finally, experiments performed at higher loading conditions (30 and 40 K) show larger intensities of the 4091 cm^{-1} IR band at 40 than 30 K; however, larger intensities are observed at 30 than at 40 K for the IR band at 4133 cm^{-1}. Part of the reason is that sites with lower binding energies can be occupied. In general, the pressure and temperature dependence of integrated areas indicates that there are variations in IR shifts and dipole moment changes as more hydrogen is loaded into the MOFs. All these effects will be discussed in the following section.

5. Discussion

To understand the interaction of H_2 with MOF systems, it is helpful to summarize the properties of the hydrogen internal modes, the H_2 stretch band, which is a sensitive measure of H_2 interactions with a host material. Free hydrogen molecules are IR inactive as other homonuclear diatomic molecules due to their lack of dipole moment. IR activity is induced through interaction with a polarizing center. The H_2 molecules exist as two isomers with different nuclear spin: *para*-H_2 characterized by a nuclear singlet state ($I = 0$) and *ortho*-H_2 characterized by a nuclear triplet state ($I = 1$). The two states have different rotational transitions dictated by the selection rules: between even J (rotational quantum number) values for *para*- and between odd J for *ortho*-H_2. The purely vibrational transitions from $\nu = 0$ to $\nu = 1$ (ν, vibrational quantum number) for para $Q(0)$ and ortho $Q(1)$ states are at 4161 and 4155 cm^{-1}, respectively. The equilibrium compositions for ortho:para are 3:1 at 300 K and $\sim$1:99 at 20 K. The vibrational−rotational components due to quadrupolar induction are $S(0)$ at 4500 cm^{-1} for *para*-H_2 and S(1) at 4715 cm^{-1}.[50]

In general, the shift in H_2 stretch frequency from the unperturbed value can be associated with the interaction at a specific binding site. For MOF-74, the highest energy binding site is the site closest to the unsaturated metal center, as shown by neutron scattering[33] and also confirmed here. The temperature at which H_2 is loaded into activated MOF-74-M systems has a large effect on the occupation of the sites. At room temperature and high pressures, H_2 can diffuse through the whole sample, and the overall loading is low (<1/10th saturation at 45 kTorr). Consequently, the highest adsorption energy sites are preferentially occupied, in this case, the metal sites. At very low temperatures (15 K or below), H_2 cannot diffuse deep into the bulk of the MOF because of lack of mobility. Moreover, H_2 can only occupy sites that have no (or very low) activation barriers, that can be overcome at such low temperatures.

Table 2. Calculated Stretching Frequency Shifts (in cm^{-1}) for H_2 Adsorbed in MOF-74-Zn/Mg at Four Different H_2 Loadings

loading	metal site Zn/Mg	O site Zn/Mg	C6H6 site Zn/Mg	center site Zn/Mg
$1H_2$/unit cell	−39/−51			
$12H_2$/unit cell	−60/−67	−41/−45		
$18H_2$/unit cell	−42/−52	−43/−40	−16/−30	
$24H_2$/unit cell	−45/−54	−38/−35	−12/−27	−32/−32

5.1. Isolated H_2 at the Metal Site (H_2^M). For MOF-74, isotherm measurements performed at room temperature and high (45 kTorr) pressure yield ∼1 H_2/primitive unit cell (1/6 H_2/M), indicating that the majority of the hydrogen molecules reside at the metal site with a statistically negligible occupation of the oxygen sites (see Supporting Information Figure S1 for MOF-74 structure and the discussion below).[77] Therefore, an important result of this work is that the shift associated with H_2 molecules isolated at metal sites denoted as H_2^M is ∼ −30 cm^{-1} at room temperature for MOF-74-Zn and ∼ −32 cm^{-1} for MOF-74-Mg. The fact that the same site is occupied at 15 K as at room temperature indicates there is no barrier to access this high binding energy site (i.e., the metal site). These IR shifts are smaller than what was observed (∼ −38 cm^{-1}) for 3-D pore saturated metal center Zn(bdc)(ted)$_{0.5}$ with lower binding energies of ∼5.3 kJ/mol.[52,65] This clearly indicates that IR shifts do not correlate with binding energies but rather with the environment of adsorbed H_2.

There appears to be a weak dependence on the metal center, in contrast to MOFs with saturated metal centers.[52] As summarized in Table 1, room temperature and high pressure measurements performed on MOF-74-M show a weak (∼4 cm^{-1} at 300 K) dependence of IR shifts on the nature of the unsaturated metal center. The largest IR red shifts correspond to metal centers with the largest binding energies (shortest M-H_2 distance). There is also some dependence of the integrated intensities of the main υ(H−H) IR absorption band for the different MOF-74-M. Figure 3 shows that, while there is a linear dependence on pressure, the magnitude of the absorption is higher for Mg (and Ni) than for Zn, which is consistent with uptakes shown by isotherm measurements at 77 K.[34]

The main observation at 300 and 15 K is that occupation of the isolated metal site leads to shifts that are smaller than what was previously reported when measured at 40 K or loaded at room temperature and then cooled to 77 or 40 K.[43,60] To understand this and other observations, we now turn to vdW-DF calculations.

5.2. Shifts of H_2 in Various Binding Sites and Evidence for H_2−H_2 Pairing. Neutron scattering measurements have shown that there are four types of binding sites in MOF-74,[33] which are, in order of binding strength, the metal site, oxygen triangle site, benzene site, and center site as shown in Figure S9 in the Supporting Information. Each of these sites has a multiplicity of six per primitive cell due to the 3-fold rotation and inversion symmetry of the structure. These observations are also confirmed by vdW-DF calculations.[64] Here, we calculate the stretching frequency shift of H_2 at these adsorption sites for four different loadings (1, 12, 18, and 24 H_2 per primitive unit cell), as summarized in Table 2 for MOF-74-Zn and Mg. For the loading of 1 H_2/cell, only one of the six metal sites is occupied. The other three loadings represent the high symmetry conditions where each type of binding site is either fully occupied or empty. The occupation order is that the stronger binding sites always get filled first before occupying the weaker binding sites. We emphasize that the experiments probably correspond to intermediate loadings, such as 3 or 10H_2/primitive cell, which is different from what we calculate here, except for the limiting cases such as very low loading (metal site occupation only) or very high loading with all sites occupied. Accordingly, the calculated and the measured frequencies may be different and cannot be compared directly for those intermediate loading conditions. However, as will be demonstrated, the important features are captured by these calculations.

Table 2 shows that the frequency shift of isolated H_2 at the metal site in MOF-74-Zn (1H_2/primitive unit cell) is −39 cm^{-1}, in good agreement with the measured −30 cm^{-1}. The calculated frequency for MOF-74-Mg is −51 cm^{-1}, which is not in as good an agreement with the observed value of ∼32 cm^{-1}. As mentioned before, we used the experimental structure for MOF-74-Zn, which is partly justified by the good agreement between the calculated binding energy, para−ortho transition energies, and the measured Q_{st} and inelastic neutron scattering data,[64] while the MOF-74-Mg structure was relaxed by GGA with experimental lattice constant. The large difference between the calculated and measured H_2 frequency shifts in MOF-74-Mg may therefore be due to the difference between our GGA-relaxed structure and the experimental structure. More importantly, the calculations show that the shift associated with H_2 at the metal site increases by 21 cm^{-1} for MOF-74-Zn (16 cm^{-1} for MOF-74-Mg) when the oxygen site is occupied, from −39 to −60 cm^{-1} (−51 to −67 cm^{-1}). This increase of the shift persists for both the "as-is" and relaxed structures and suggests that there is some interaction between H_2 at the metal site and H_2 at the oxygen site. Such interaction is not surprising, because the neutron diffraction experiments indicate that the H_2−H_2 distance is only 2.9 Å, which is close enough to be described as a H_2−H_2 pair.[33] Indeed, the theory predicts that the oxygen site is unstable unless the corresponding Zn site is occupied.

Thus, another important finding of this work is that the mode observed at ∼4090 cm^{-1}, that is, featuring a large (∼ −70 cm^{-1}) shift from the unperturbed H_2 stretch frequency, is associated with H_2 at metal site only when the oxygen site is occupied, that is, when "pairing" occurs, denoted by H_2^{M-O}. While population of the isolated metal site H_2^M does not require activation energy because it is occupied at 15 K (see Figure 3), the situation is different for the oxygen site. At 15 K, there is little contribution at 4091 (4093) cm^{-1} over most pressures, indicating that the oxygen site cannot be completely occupied. However, if the loading is performed at 30 or 40 K (Figure 7), the intensity of the 4091 cm^{-1} band is larger. Alternatively, this band dominates when the sample is loaded at room temperature and then cooled (Figure 5) or loaded at 77 K (Figure 6). The ability to incorporate more H_2 (recognized here as populating both the metal and oxygen sites) by starting at room temperature is the reason why this procedure has been implemented by many groups for the study of adsorption into MOFs.[42,43]

The presence of a weak shoulder at ∼4100 cm^{-1} at 300 K (Figure 1) and the dominance of this band (∼4091 cm^{-1}) at 77 K even at the lowest pressures (with absence of the absorption band of H_2^M) suggest that the occupation of these two sites (metal and oxygen sites) may stabilize the system, at least for intermediate loadings when there are only a few H_2 in each primitive unit cell. The linear behavior of isotherms performed at room temperature indicates that at these conditions the loading is influenced heavily by isolated H_2 adsorbed at the metal site. There is therefore no change in binding energy.[77] However, isotherms preformed by Liu et al.[33] at 77 K for MOF-74-Zn

show a sharp increase in uptake in the low pressure regime (Henry's law region), indicating a high adsorption enthalpy in that region. At the lowest pressure (7.5 Torr), there are only $\sim$2.5H_2/primitive cell. The inhomogeneous occupation of the metal sites at 77 K, due to kinetic limitations that favor "pair" formation, would lead to the unexpected dependence of Q_{st} on loading as the loading increases as shown by Rowsell et al.[36] and Liu et al.[33] These groups have shown that there is an unusual behavior in the binding energies of MOF-74 derived from isotherm measurements at low loading. This observation was tentatively attributed to H_2-H_2 interactions.[33,36] The results presented above support the concept that diffusion barriers causing pairing could explain these differences.

The vdW-DF theory is not able to determine whether the paired state is the lowest energy state, as is suggested by the data obtained at 77 K. In the current calculations, the paired state energy is $\sim$10% higher (i.e., less bound) per H_2 than the energy of isolated H_2 at the metal site, an amount that is smaller than the expected accuracy of the theory. Because the H_2-H_2 attraction within vdW-DF is known to be too strong at the pairing distance, it is quite possible that the paired energy is even higher or less bound.

The interpretation of inelastic neutron scattering indicates that for D_2 the loading is sequential, which would indicate that for D_2 there is no pairing.[33] A more definitive confirmation that pairing stabilizes H_2 even further is therefore needed because it is unfortunately not possible to study D_2 with IR spectroscopy at present (due to interference from the MOF lattice absorption in the D_2 stretch absorption region ($\sim$2900$-$3000 cm^{-1})). In such a comparison, it is important to reproduce loading conditions exactly because kinetic factors can affect the occupation sequence.

The measurements performed at low pressures and temperatures (15$-$40 K) suggest that H_2 pairs are formed by occupation of both the metal and the oxygen sites, when the temperature is high enough (>30 K) to overcome the pair formation energy. As discussed below, the spectra in Figure 7 show that the intensity of the 4091 cm^{-1} band is much higher at 40 than 30 K at similar pressures, which is consistent with the need for thermal activation to occupy the oxygen site and thus make a pair. Figures 8 and 9 also show that at a given temperature and pressure, this band increases with time with a dependence with which such an equilibrium cannot be reached at 30 K within reasonable times (<many hours) and still requires $\sim$2 h at 40 K.

These conclusions contrast those of earlier studies, which attributed the large shift (~ -70 cm^{-1}) from the unperturbed υ(H$-$H) to H_2 at the primary adsorption site "unsaturated metal center" based on standard correlation between binding energies and IR shifts. Consequently, the less shifted ~ -30 cm^{-1} IR bands observed at low temperatures ($T < 78$ K) were attributed to lower binding energy adsorption sites such as "oxygen" and "benzene" sites, ignoring the effects of each adsorption site on another.[42,43] A recent IR study on H_2 adsorption in MOF-74 had similar conclusions[60] and attributed small shifts (~ -2 cm^{-1}) to H_2-H_2 interactions, which is lower than what is calculated here.

5.3. Variation in H_2 Stretch-Induced Dipole Moments. Another important finding of the theoretical calculations is that the induced dipole moments of H_2 adsorbed in MOF-74-M can vary substantially as a function of loading, as summarized in Table 3 for MOF-74-Zn and Mg metal centers where the derivative of the induced dipole moment with respect to H_2 bond stretching (i.e., effective charge as defined in eq 2) is shown. Four H_2 loading conditions were considered in Table 2. We again emphasize that the experimental data probably correspond to intermediate loadings and may therefore not be directly compared to the calculated values.

Table 3. Calculated Effective Charge (the Derivative of Dipole Moment with Respect to H_2 Bond Stretch, As Defined in Eq 2) for H_2 at Various Binding Sites in MOF-74-Zn/Mg (Units of $10^{-2}e$)

loading	dipole moment metal site Zn/Mg	dipole moment O site Zn/Mg	dipole moment C6H6 site Zn/Mg	dipole moment center site Zn/Mg
1H_2/unit cell	3.5/4.1			
12H_2/unit cell	2.9/3.0	4.2/4.8		
18H_2/unit cell	5.1/4.1	3.7/4.2	2.3/3.0	
24H_2/unit cell	5.6/4.4	4.6/4.7	2.4/3.8	1.4/1.3

Although the accuracy of the calculations for the dipole moment is low, the results listed in Table 3 confirm that large variations are taking place as the loading changes. In particular, the effective charge of H_2 on the Mg site decreases from 0.021e to 0.015e as the loading increases from 1 to 12 H_2/primitive cell. Therefore, the IR intensity is reduced by $\sim$50% because it is proportional to the square of the effective charge or dynamic dipole moment. The large change in effective charge is due to interactions between two H_2 molecules at the Mg and the oxygen sites, as suggested by the frequency change shown in Table 2. It is also expected that the dipole moments can vary for partial loadings between these high symmetry loadings of 12, 18, and 24 H_2 per primitive cell. These findings show that possible variations in dipole moment have to be taken into account when interpreting the IR intensity as a function of loading. One important consequence is that the commonly used VTIR method for determining adsorption energy should be used with caution when there is interaction between adsorbed molecules.[51,79]

5.4. Higher Loadings. The interpretation of IR data at higher loadings is more difficult and speculative because of lack of uptake information at these temperatures. Tables 2 and 3 for MOF-74-Zn and -Mg clearly show large variations in frequency shifts (Table 2) and dipole moments (Table 3) as a function of H_2 loading. As noted above, the IR band of H_2 adsorbed on the metal site undergoes a sizable red shift (-21 for Zn and -16 cm^{-1} for Mg) when the H_2 pair is formed (at 12 H_2/unit cell), but returns to within 3$-$1 cm^{-1} of its original position when the benzene site is occupied (18 and 24 H_2/unit cell). It is also apparent that all other sites (oxygen, benzene, and center sites) have similar shifts (within 13 cm^{-1}) and may therefore be hard to distinguish. Dipole moment calculations also show quite complex variations as a function of loading.

The IR spectra at 15 K shown in Figure 3 reveal that at these temperatures H_2 (characterized by a band in the 4129$-$4135 cm^{-1} range) is mostly occupying the metal site, similarly to the situation at room temperature. In contrast, IR spectra collected at higher temperatures (40 or 77 K) are dominated by a band centered at 4091 cm^{-1}, as shown in Figures 6 and 7b. As described above, this band is associated with H_2 at the metal site when the oxygen site is occupied $\nu(H_2^{M-O})$. It is clearly much weaker at 30 K (Figure 7a). Therefore, the formation of this H_2-H_2 pairs probably requires a higher sample temperature ($\sim$40 K). Assuming reversibility, this observation is consistent

(79) Arean, C. O.; Manoilova, O. V.; Palomino, G. T.; Delgado, M. R.; Tsyganenko, A. A.; Bonelli, B.; Garrone, E. *Phys. Chem. Chem. Phys.* **2002**, *4*, 5713–5715.

with the results of an earlier inelastic neutron scattering study[33] that noted that temperature had to be raised to 50 K (i.e., >30 K) to remove H_2 at the oxygen site when the system is being pumped on. We can therefore draw the conclusion that the kinetic barrier for H_2-H_2 pairing corresponds to ~40 K (~0.5 kJ/mol).

Kinetic issues are still important in the 30−40 K range and need to be taken into account as the nature of the broad 4133 cm^{-1} band is considered. At both 30 and 40 K, hydrogen molecules cannot penetrate fully into the microcrystals. This conclusion is reached by comparing the total integrated areas of the 4091−4093 cm^{-1} bands at 77 K (Figure 6), 30 K (Figure 8a), and 40 K (Figure 9a). Hydrogen atoms inside the pores located close to the periphery of the microcrystals prevent further penetration at low temperatures. Given this situation, the time dependence of the spectra at 30 K (Figure 8b) and 40 K (Figure 9b) is composed of both occupation of sites within a pore due to the continued penetration of H_2 within the microcrystal and ortho−para conversion (~ +6 cm^{-1} blue shift). Furthermore, the broad band at 4133 cm^{-1} consists of several components as detailed in Figure S6 (Supporting Information), which renders the interpretation of its pressure, time, and temperature dependence more difficult.

Starting our discussion with the 40 K case and looking at the differential spectra shown in Figure 9b, the intensity loss at ~4125 cm^{-1} (seen as a negative feature at ~4120 cm^{-1} because of a gain at higher frequencies) and a corresponding gain at 4091 cm^{-1} ($\nu(H_2^{M-O})$) is due to the occupation of the oxygen site and the formation of H_2 pairs. As shown in Table 2 summarizing the theoretical calculations, the formation of H_2 pairs causes a shift in frequency of H_2 adsorbed at the metal site from $\nu(H_2^{M})$ at ~4125 cm^{-1} to $\nu(H_2^{M-O})$ at 4091 cm^{-1} due to H_2-H_2 interactions. This effect is most apparent in Figure 10 where there is an increase in the 4091 cm^{-1} IR band accompanied by a sharp decrease in the 4133 cm^{-1} band.

At 30 K, the situation is more complicated than at 40 K due to kinetic limitations. Time-dependent IR spectra shown in Figure 8b show that there is no significant change of the IR band centered at 4091 cm^{-1}; there is instead a decrease in the intensity of the IR band centered at 4121 cm^{-1}. The integrated area of the IR band at 4091 cm^{-1} (Figure 10a) appear to be smaller than that at 40 K. This indicates that, under these conditions, most of the oxygen sites are not occupied due to slow diffusion and for lack of sufficient energy to overcome the activation barrier for H_2 pairing to occur. Therefore, the majority of the contribution toward the IR band centered at 4133 cm^{-1} is due to H_2 isolated at the metal site. Note that this band becomes stronger than at 40 K. This is due to a number of factors. First, there are relatively more H_2's isolated at the metal site (~4125 cm^{-1}) than at 40 K because the oxygen site cannot be easily occupied. Second, some of the MOF's unit cells at the periphery could have higher loadings with the occupation of the benzene site. The continued occupation of the oxygen and benzene sites at the peripheries and the reversion of the IR band correlated to H_2 adsorbed at the metal site due to the benzene site occupation both lead to an overall larger integrated area of the band centered at 4133 cm^{-1}.

Table 4 summarizes the possible assignments for the main experimental observations for both Zn and Mg MOF-74 discussed above. The differences between the Zn and Mg MOF-74 are small enough that the ranges for each species are not distinguishable. The frequencies are shown in a range to include the complicating factors of ortho−para conversion (~6 cm^{-1} and a blue shift of ~7 cm^{-1} for H_2 liquefaction at 15 K) that lead to frequency shifts as a function of time at a specific temperature.

Table 4. Summary of Adsorption Sites and Corresponding Measured Frequencies for Both Zn and Mg Metal Center MOF-74

adsorption site	loading temperature [K]	measured frequency range Zn, Mg [cm^{-1}]	dipole moment
isolated H_2 M^{+2}	15, 30, 40, and 300-high pressure	4125−4138 4125, 4123	strong
M^{+2} when O site occupied	30, 40, 77, 300	4087−4093, 4084−4091	medium
M^{+2} when benzene site occupied	30, 40	4125−4135	medium
oxygen	30, 40, 77, 300	4118−4122	weak
benzene	30, 40, 77, 300	4127−4143	medium

Effect of Occupation of the Different Sites on Adsorbed H_2 Dipole Moment. The difference in integrated areas between the IR bands centered at (i) 4091 cm^{-1} due to H_2 adsorbed on the metal site when the oxygen site is occupied (H_2^{M-O}) and (ii) 4133 cm^{-1} due to isolated H_2 adsorbed at the metal site (H_2^{M}) and other sites shown in Figure 10b at 40 K suggests that the dynamic dipole moment of H_2 at the metal site weakens upon occupation of the secondary "oxygen" site H_2^{O}. This is in good agreement with the theoretical calculations showing that the dynamic dipole of the H_2 at the metal site weakens when the oxygen site (for $12H_2$/primitive unit cell) is completely occupied in the unit cell as shown in Table 3. As mentioned above, the band at 4133 cm^{-1} dominates at 30 K for two reasons: occupation of the metal site by isolated H_2 throughout the sample particularly deep inside the microcrystals, then occupation of the oxygen and benzene sites at the periphery of the sample. The near surface (peripheric) region is able to incorporate higher H_2 loading than at 40 K, hence the more sustained pressure dependence. As mentioned before, this band is composed of many components, including a feature at 4118 cm^{-1} due to H_2 adsorbed at the oxygen site as shown in Figure S5 (Supporting Information). The dipole moment of this band decreases with loading as indicated by the theoretical calculations shown in Table 3. Therefore, the gradual intensity decrease of the band centered at 4133 cm^{-1} as the pressure is increased is due to the weakening of the dipole moment of H_2 adsorbed at the oxygen site H_2^{O} as the benzene site is occupied. The experiment performed to test whether a low binding energy site is occupied and does contribute to the 4133 cm^{-1} band (summarized in Figure 11) confirms the occupation of the benzene site. Note that in this particular case, this site contributed to ~1/2 of the total integrated area of the 4133 cm^{-1} band. The other half remains present, even after extensive time in high vacuum, confirming that a more tightly bound H_2 (isolated at the metal site) is present. The slight increase in integrated area of H_2 at 4091 cm^{-1} band confirms that there is variation in dipole moment of this band as the benzene site is occupied (i.e., loss of H_2 at the benzene site increases the dipole moment of H_2 at the metal site).

The main conclusion from this section is that, at low temperatures (<40 K), the situation is complicated by several factors. First, the loading of the microcrystallites is not uniform with little H_2 deep inside and highest loading at the periphery. Second, the band at 4133 cm^{-1} arises from H_2 at several locations (isolated H_2 at the metal center, H_2 at the oxygen,

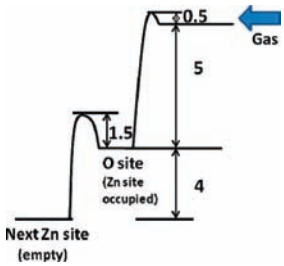

Figure 12. Hypothetical schematic potential energy curve on an optimal path from the gas phase (right) to an oxygen site (center) with the neighboring Zn site occupied (i.e., to form a pair), and then to the next empty Zn site (left). The H_2 at the Zn sites are taken to be bound by ~9 kJ/mol, and the one at a paired oxygen site is bound by ~5 kJ/mol. The two barriers of ~0.5 and ~1.5 kJ/mol are suggested by our measurements and discussed in the text.

benzene, and possibly center sites). Third, the occupation of the oxygen site requires thermal activation, while the occupation of the benzene site may require occupation of the oxygen site. All these factors make it very difficult to extract unambiguous information in the 15−40 K temperature range.

5.5. Proposed Simplistic Model. To better visualize the suggested mechanism proposed above, we describe here a simplistic, semiquantitative model (i.e. not supported by calculations) that can describe the main observations and highlights the main hypotheses. Four assumptions are derived from the observations and summarized in Figure 12.

(1) After the metal site is occupied (binding energy ~9 kJ/mol for H_2 at that site), there is an activation barrier of ~0.5 kJ/mol to occupy the neighboring oxygen site, that is, to form a pair. The magnitude of this barrier is chosen from the observation that "pairs" cannot form at temperatures below 40 K. Physically, this barrier may arise for the need of the incoming molecule to orient itself properly to achieve the highest binding energy configuration.

(2) With the nearby metal site occupied, the binding energy for a H_2 at the oxygen site is ~5 kJ/mol as suggested by Q_{st} measurements.

(3) At temperatures below 80 K, there are kinetic limitations that lead to higher loading in the periphery of the MOF than deep inside the MOF. This assumption is based on the observations that (i) the integrated areas are lower at low temperatures than at room temperature, (ii) the intensities of the H_2 bands are time dependent, and (iii) the data at low temperature indicate higher loading than expected on the basis of external pressures. Physically, this assumption implies that H_2 molecules migrate through the MOF via diffusion (i.e., sampling potential binding sites) rather than ballistically. This diffusion involves sampling all the possible sites, including those already occupied by H_2 molecules, such as H_2 at the metal sites, starting from the surface of the MOF.

(4) We assume that the barrier for the above migration of the H_2 on the oxygen site (with the corresponding metal site occupied, that is, the paired configuration) to another empty Zn site is ~1.5 kJ/mol, a value estimated from our measurements at 77 K. The interaction between the paired H_2's should make a contribution to this barrier. A schematic plot of the hypothesized potential energy curve along the optimal path from the gas phase outside the MOF to the oxygen site (pairing) to another Zn site is shown in Figure 12.

With these assumptions, it is clear H_2-H_2 pairs can be formed at 77 K (~0.7 kJ/mol) because the formation barrier (~0.5 kJ/mol) is overcome. The pairs preferentially form at the periphery of the MOF because of diffusion kinetics. Moreover, these pairs can be stabilized at 77 K because the disruption energy barrier (~1.5 kJ/mol) is higher than the thermal energy (~0.7 kJ/mol).

The purpose of this model is to illustrate that the main observations presented in this Article can be accounted for. We emphasize that this model has not been examined by first principles calculation and does not address uniqueness for these mechanisms. It is provided as a potential guide to think about this system and a simplified summary of our observations.

6. Conclusions

This work examines H_2 interactions with the unsaturated metal center in MOF-74-M (where M = Zn, Mg) combining infrared absorption spectroscopy and vdW-DF calculations. Evidence for H_2-H_2 interactions and formation of H_2 "pairs" on adjacent adsorption sites is obtained. Surprisingly small IR shifts (~ -30 cm^{-1}) are observed for H_2 adsorbed on the unsaturated metal center site. An additional ~ -32 cm^{-1} IR shift and strong dipole moment changes are observed and attributed to effects caused by H_2-H_2 interactions.

IR shifts due to H_2 adsorbed on the unsaturated metal site with higher binding energies (~10 kJ/mol) are found to be smaller than what was observed for the saturated metal center $Zn(bdc)(ted)_{0.5}$ (~ -38 cm^{-1}) with lower binding energies (~4 kJ/mol).[52] This observation suggests that IR shifts do not correlate with binding energies, similarly to what was observed in a recent IR study for saturated metal center MOFs.[52] The shift depends mostly on the chemical environment of H_2, not its binding energy. While there may be a small dependence on the metal atom, hence possibly binding energy (observed at room temperature and high pressure), these shifts ($\sim \pm 4$ cm^{-1}) are similar to shifts caused by metal exchange in 1-D pore structure MOFs with aliphatic ligands ($M_3(COOH)_6$), which were attributed to structural changes causing a change in adsorption environment.[52]

In contrast to the assumption made in earlier studies,[42−60] the dynamic dipole moment and the frequency of adsorbed H_2 appear to be greatly affected by H_2-H_2 interactions with the loading of neighboring sites. For instance, the dipole moment of H_2 adsorbed onto the unsaturated metal site weakens with the occupation of the secondary oxygen site and the formation of H_2 pairs. Moreover, its frequency red shifts substantially (the shift increases by ~ -30 cm^{-1}) when the H_2 pair is formed due to H_2-H_2 interactions. Furthermore, spectroscopic data suggest that, when there is complete occupation of the three highest binding energy adsorption sites, the dynamic dipole moment of H_2 adsorbed on the secondary "oxygen site" weakens and the frequency of H_2 at the metal site shifts back to its value when isolated (by $\sim +30$ cm^{-1}).

Finally, we have shown that integrated areas of specific IR bands do not always correlate with the amount of H_2 adsorbed. The dynamic dipole moment of adsorbed H_2 on proximate adsorption sites appears to be dependent on the occupation of neighboring sites (i.e., weakening of the dynamic dipole moment of H_2 adsorbed on the metal site when the oxygen site is occupied). Therefore, caution must be implemented when using the variable temperature IR (VTIR) method to calculate adsorption energies at specific adsorption sites.

A simple model is presented to summarize the observations, which suggests that there is a small activation barrier for the formation of H_2-H_2 "pairs" and a slightly larger energy for the hydrogen on the oxygen site to go to the next empty metal

site. This model also invokes kinetic limitation for the incorporation of H_2 deep inside the MOF crystals.

Acknowledgment. This work is supported in full by the Department of Energy (DOE Grant No. DE-FG02-08ER46491).

Supporting Information Available: Crystal structures of MOF-74-M (M = Zn, Mg, Ni) series in as-synthesized and dehydrated state; high pressure IR data for MOF-74-Ni; IR spectra of H_2 adsorbed at 15 K for MOF-74-Mg; fitting of IR spectrum at 2 Torr and 40 K; integrated areas of H_2 adsorption at 77 K for MOF-74-Zn and Mg and adsorption−desorption isotherms performed at 77 K; lower pressure IR spectra of H_2 adsorbed in MOF-74-Zn and Mg at 77 K and a larger frequency range of IR spectra at 30 and 40 K for MOF-74-Mg; a figure showing the different adsorption sites in MOF-74; and X-ray diffraction and TG analysis of the studied MOFs. This material is available free of charge via the Internet at http://pubs.acs.org.

JA104923F